Biochemical Society Transactions (2020) **48** 1765–1780
https://doi.org/10.1042/BST20200243

Review Article

The structural biology of canonical Wnt signalling

Mark Agostino[1,2] and Sebastian Öther-Gee Pohl[1,3]

[1]School of Pharmacy and Biomedical Sciences, Curtin Health Innovation Research Institute (CHIRI), Curtin University, Bentley, Western Australia, Australia; [2]Curtin Institute for Computation, Curtin University, Bentley, Western Australia, Australia; [3]The Institute of Genetics and Molecular Medicine, Edinburgh Cancer Research Centre, University of Edinburgh, U.K.

Correspondence: Mark Agostino (Mark.Agostino@curtin.edu.au) or Sebastian Öther-Gee Pohl (Sebastian.pohl@igmm.ed.ac.uk)

The Wnt signalling pathways are of great importance in embryonic development and oncogenesis. Canonical and non-canonical Wnt signalling pathways are known, with the canonical (or β-catenin dependent) pathway being perhaps the best studied of these. While structural knowledge of proteins and interactions involved in canonical Wnt signalling has accumulated over the past 20 years, the pace of discovery has increased in recent years, with the structures of several key proteins and assemblies in the pathway being released. In this review, we provide a brief overview of canonical Wnt signalling, followed by a comprehensive overview of currently available X-ray, NMR and cryoEM data elaborating the structures of proteins and interactions involved in canonical Wnt signalling. While the volume of structures available is considerable, numerous gaps in knowledge remain, particularly a comprehensive understanding of the assembly of large multiprotein complexes mediating key aspects of pathway, as well as understanding the structure and activation of membrane receptors in the pathway. Nonetheless, the presently available data affords considerable opportunities for structure-based drug design efforts targeting canonical Wnt signalling.

Brief overview of canonical Wnt signalling

Wnt signalling involves a series of complex pathways and underpins developmental processes [1]. When dysregulated, it is synonymous with impaired regeneration and a variety of pathological states, including carcinogenesis [2–5]. Wnt signalling is primarily classed into canonical (β-catenin dependent) and non-canonical (β-catenin independent) pathways. Canonical Wnt signalling is primarily controlled through the regulation of three distinct multiprotein complexes: the signalosome, the degradosome and the nuclear enhanceosome, as well a variety of extracellular agonists and antagonists which precede these intracellular events [6] (Figure 1).

Wnt signalling can be initiated or enhanced by a variety of extracellular ligands, including Wnt and Norrin proteins, which bind to Frizzled (Fzd) receptors, and R-spondins (RSPOs), which bind to LGR family receptors. Wnt proteins are lipid-modified at a conserved serine by the *O*-acyltransferase Porcupine to facilitate secretion and receptor binding. Canonical Wnt signalling can be amplified following concomitant binding of Wnt and R-spondin (RSPO) ligands, which may function dependently or independently of LGR [7]. RSPOs prevents Fzd degradation by blocking the activity of the RING finger ubiquitin ligases, RNF43 and ZNRF3 [8,9]. Norrin is an atypical Wnt ligand that can bind specifically to Fzd4 and LRP5/6 [10], as well as the Fzd4–Tspan12 complex, to activate Wnt signalling [11]. Extracellular antagonists include Wnt inhibitory factor (WIF), secreted-Frizzled related proteins (sFRPs), Dickkopfs (DKKs) and Notum, each of which are diverse in structure and function (specific details of which will be elaborated later in the review). Wnt ligand binding to membrane-bound receptors and co-receptors results in the formation of multiprotein assemblies or 'signalosomes', composed of Fzd receptors and LRP5/6 co-receptors bound to Wnt ligands. These signalosomes are highly dynamic and can be negatively regulated by RNF43/ZNRF3, which, in turn, is balanced by R-spondin–LGR5 receptor interactions [12].

Received: 26 May 2020
Revised: 4 July 2020
Accepted: 7 July 2020

Version of Record published: 29 July 2020

Biochemical Society Transactions (2020) **48** 1765–1780
https://doi.org/10.1042/BST20200243

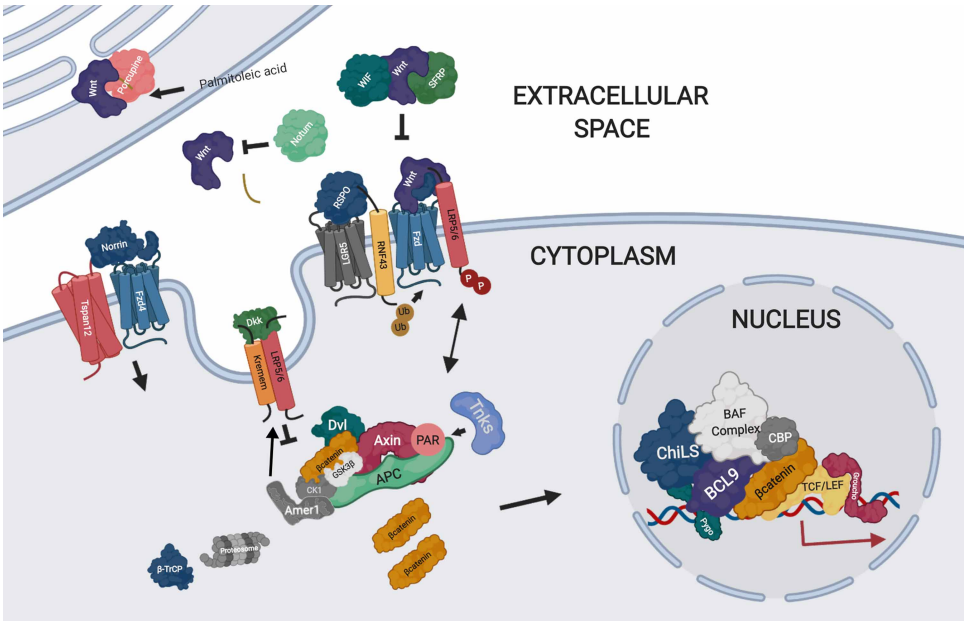

Figure 1. Graphical overview of canonical Wnt signalling.
Figure prepared using BioRender.

Intracellularly, Wnt signalling is controlled at the level of the β-catenin destruction complex, or the degradosome, which primarily consists of the scaffold protein Axin, glycogen synthase kinase 3β (GSK3β), casein kinase 1α (CK1α), protein phosphatase 2A (PP2A) and Adenomatous Polyposis Coli (APC). [13] In the absence of Wnt stimulation, β-catenin is sequentially phosphorylated by CK1α (Ser45) and GSK3β (Thr41, Ser37, Ser33), resulting in ubiquitin-mediated proteasomal degradation through a β-TrCP-dependent mechanism. Following Wnt stimulation, the degradosome is recruited to the membrane through a Dvl-Axin mediated mechanism, where phosphorylation of the co-receptor LRP5/6 on its cytoplasmic tail by GSK3β and CK1α/ε occurs [13]. The recruitment of GSK3β/CK1 and Axin can be mediated by adenomatous polyposis coli membrane recruitment 1 (Amer1) [14]. This, in turn, can result in the inhibition of GSK3β [15–18] and the translocation of β-catenin to the nucleus. Poly(ADP-ribosyl)ation of Axin by Tankyrase mediates its ubiquitination and subsequent degradation, destabilising the destruction complex, and thus activating Wnt signalling [19]. Once localised to the nucleus, β-catenin acts a co-factor for the initiation of the transcription of Wnt target genes [2]. This Wnt-driven transcriptional program is controlled by the Wnt enhanceosome, the core of which is made up of the ChiLS (Chip-SSDP/LIM-domain binding protein) complex, which binds Pygopus, Groucho/TLE and scaffold protein BCL9/legless [20,21]. In a 'Wnt off' context Groucho/TLE binds TCF/LEF and ChiLS to repress transcription, while in a 'Wnt on' environment, β-catenin induces an enhanceosome complex rearrangement to bind to TCF/LEF transcription factors, and other transcriptional co-activators (e.g. CREB-binding protein and BAF complex) to initiate target gene expression [22].

Structural knowledge of extracellular regulation of Wnt signalling

Wnts and related proteins

The structures of a relatively limited number of Wnt protein family members have been solved (Figure 2A). This is due in part to the presence of *O*-lipidation at a conserved serine that makes Wnt proteins highly hydrophobic and challenging to purify. The first structure of a Wnt protein solved was the *Xenopus* Wnt8 in complex with the mouse Fzd8 cysteine-rich domain (CRD), revealing a novel protein fold and the importance of lipidation for direct binding of Fzd [23]. This structure further illustrated that Wnts bind to Fzds at two distinct sites on opposite faces of the CRD. The Wnt protein family contains 19 members in mammals, however, the structure of only one mammalian Wnt has been solved experimentally [24]; further study of the Wnt

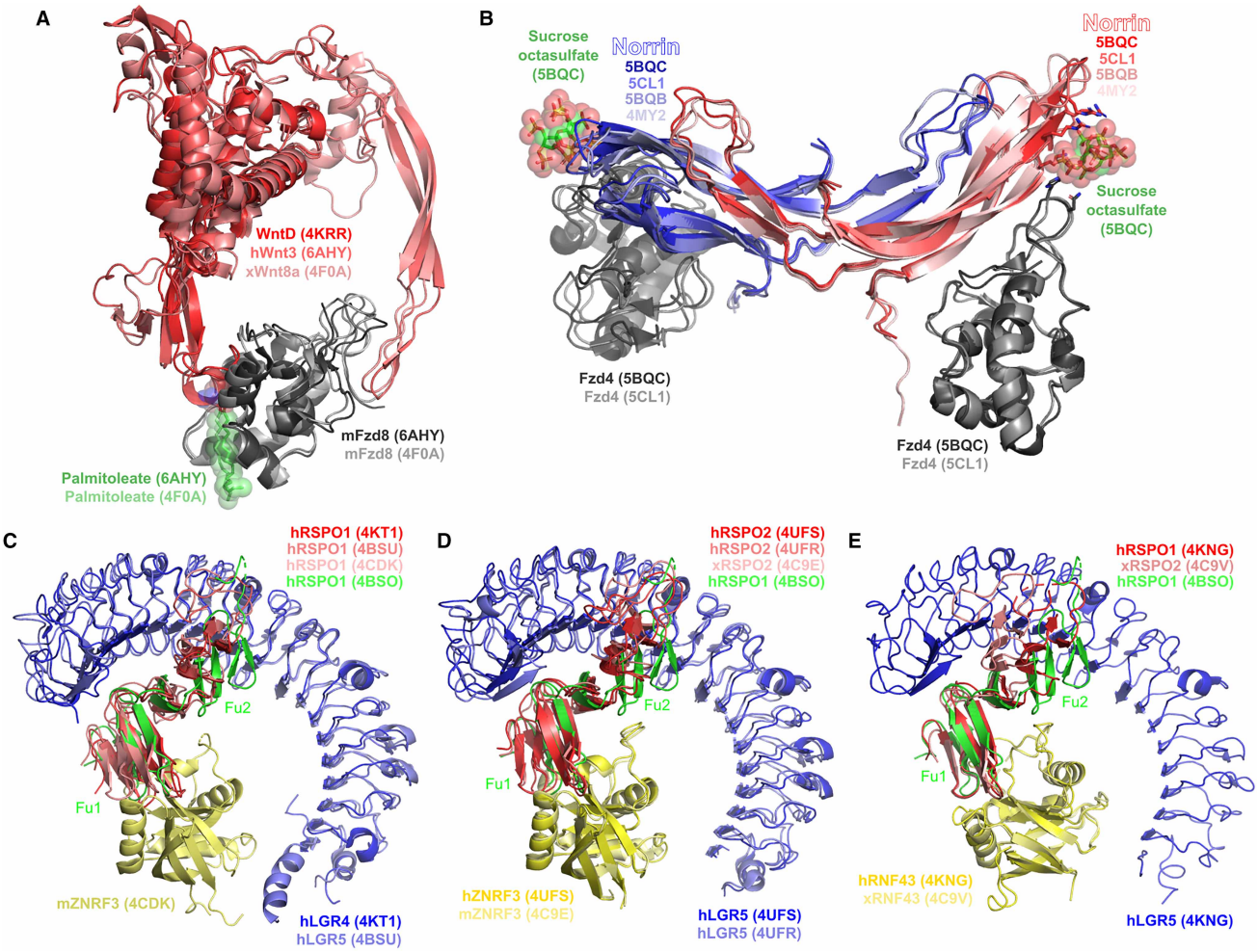

Figure 2. Structures related to interactions involving secreted positive regulators of Wnt signalling.

(**A**) Wnt-related proteins and interactions. Structures depicted include: WntD (PDB 4KRR); the human Wnt3 complex with the mouse Fzd8 cysteine-rich domain (PDB 6AHY); the *Xenopus* Wnt8a complex with the mouse Fzd8 cysteine-rich domain (PDB 4F0A). (**B**) Norrin and its interactions. Structures depicted include: unbound norrin-maltose binding protein fusion (PDB 4MY2), unbound norrin (PDB 5BQB), norrin-maltose binding protein fusion in complex with Fzd4 (PDB 5CL1), norrin-Fzd4-sucrose octasulfate ternary complex (PDB 5BQC). Maltose binding protein hidden. Key residues contacting sucrose octasulfate in PDB 5BQC are shown as sticks. (**C**) RSPO1–LGR–ZNRF3 complexes. Structure represented include: human RSPO1–LGR4 complex (PDB 4KT1), human RSPO1–LGR5 complex (PDB 4BSU), human RSPO1 in complex with mouse ZNRF3 (PDB 4CDK). The structure of native human RSPO1 (PDB 4BSO) is shown for reference. (**D**) RSPO2–LGR–ZNRF3 complexes. Structures represented include: human RSPO2–LGR5–ZNRF3 complex (PDB 4UFS), human RSPO2–LGR5 complex (PDB 4UFR), *Xenopus* RSPO2 in complex with mouse ZNRF3 (PDB 4C9E). The structure of native human RSPO1 (PDB 4BSO) is shown for reference. (**E**) R-spondin–LGR–RNF43 complexes. Structures represented include: human LGR5–RSPO1–RNF43 complex (PDB 4KNG); *Xenopus* RSPO2–RNF43 complex (PDB 4C9V). The native human RSPO1 (PDB 4BSO) is shown for reference.

family in mammals has been facilitated by computational approaches [25–27]. The structure of the N-terminal region of the *Drosophila* WntD protein revealed an overall similar fold to the N-terminal regions of other members of the Wnt family [28], although unlike other members of the family, this protein is not lipidated [29].

Norrin

Norrin is an atypical Wnt signalling activator displaying a distinct fold to Wnt, achieving its activity through forming a ternary complex with a Fzd and an LGR (Figure 2B). The first structure of Norrin obtained was that

Biochemical Society Transactions (2020) **48** 1765–1780
https://doi.org/10.1042/BST20200243

of its fusion with maltose binding protein [10]; a complex of this fusion protein with the Fzd4 CRD was subsequently obtained [30]. The structures of the unfused Norrin, its complex with Fzd4, and the Norrin-Fzd4 ternary complex with the heparin mimic sucrose octasulfate have also been determined [31], revealing the potential for glycosaminoglycans to bridge the Norrin-Fzd4 interaction. Specifically, norrin residues Lys58, Arg107, Arg109 and Arg115 and Fzd4 residues His154 and Asn155 interact directly with sucrose octasulfate in the crystal structure (Figure 2B).

R-spondins (RSPOs)

RSPOs feature two furin repeat domains (Fu1 and Fu2), as illuminated in the structures of the human RSPO1 and the *Xenopus* RSPO2 [32,33], and between which considerable flexibility is observed (Figure 2C–E). Numerous structures of RSPO1 bound to the leucine-rich repeat (LRR) ectodomains of LGR4 and LGR5 have been reported [33–35]; a structure of RSPO2 bound to the LGR5 ectodomain has also been reported [36]. In all cases, these structures feature the LRRs of the LGR ectodomain curving around Fu2 of the RSPO. Fu1 of RSPOs mediates the interaction with ZNRF3 [32–37] and RNF43 [32]. Due to the complementary utilisation of the Fu1 and Fu2 domains, ternary complexes of RSPOs, LGRs and RING finger ubiquitin ligases are possible and have been structurally characterised [36–38]. Subtle variations in how ZNRF3 and RNF43 are recognised by LGRs are observed in the crystal structures; specifically, the LRR does not appear to directly bind ZNRF3 (although in one structure, a helix immediately after the LRR is observed to bind to ZNRF3) (Figure 2C,D), while RNF43 is directly bound by the LRR, albeit weakly (Figure 2E).

Secreted Frizzled-related proteins (sFRPs)

In mammals, five sFRPs are known (sFRP1–5). These proteins feature a two-domain structure, containing an N-terminal Fzd-type CRD Frizzled-type cysteine-rich domain (CRD), and a C-terminal netrin-like domain (NLD) [39]. The exact mechanism by which sFRPs function as Wnt signalling inhibitors is still under investigation (in particular, the importance of the NLD in inhibition), but it is widely believed they act as inhibitors by binding Wnt proteins using their CRD, thus preventing the ability of Wnts to bind Fzds and initiate Wnt signalling [40]. Structural knowledge of sFRPs and related proteins is presently limited, with only two such structures reported (Figure 3): the mouse sFRP3 CRD [41] and the *Xenopus* Sizzled protein [42] (Figure 3A). The mouse sFRP3 CRD — along with the mouse Fzd8 CRD — were the first structures of Fzd-type cysteine-rich domains to be characterised. The Sizzled structure is of particular interest as it is the only structure of an sFRP-related protein to feature both the CRD and NLD, providing insight into how the two domains may co-ordinate to modulate Wnt signalling.

Wnt inhibitory factors (WIFs)

WIFs inhibit Wnt signalling by directly binding the Wnt lipid moiety, to prevent Fzd receptor binding, and prevent Wnt signalling [43]. The structure of the WIF domain of WIF-1 was initially determined by NMR, revealing an immunoglobulin-like fold and the location of the putative lipid-binding site [44] (Figure 3B). The site was subsequently confirmed by X-ray crystallography, as well as the involvement of WIF epidermal growth factor-like domains in binding glycosaminoglycans [45].

Notum

Notum is an extracellular deacetylase that removes *O*-lipidation from Wnt proteins, thus deactivating them. The structural biology of Notum has primarily been elaborated by a single extensive study [46], wherein structures of human and *Drosophila* Notum bound to *O*-palmitoleylserine, a heparin disaccharide, and the heparin analogue sucrose octasulfate were determined (Figure 3C). *O*-palmitoleylserine is bound by Notum at a hydrophobic cavity deep in the structure. Although a complex with full length Wnt was not determined, the study suggested that the formation of a Wnt-Notum complex is facilitated by heparin binding.

Dickkopfs (DKKs)

Four mammalian DKKs are known (DKK1-4). These proteins feature two CRDs of a distinct type to that found in sFRPs and Fzds, and primarily act to block canonical Wnt signalling by binding to LRP family co-receptors [47]. DKK also facilitates the Kremen-mediated endocytosis of LRP5/6 [48]. The majority of DKK structures have been determined in complex with LRPs, which will be covered later in the review. Only one structure of an isolated DKK CRD has been determined, that of the second CRD of the mouse DKK2 (Figure 3D) [49].

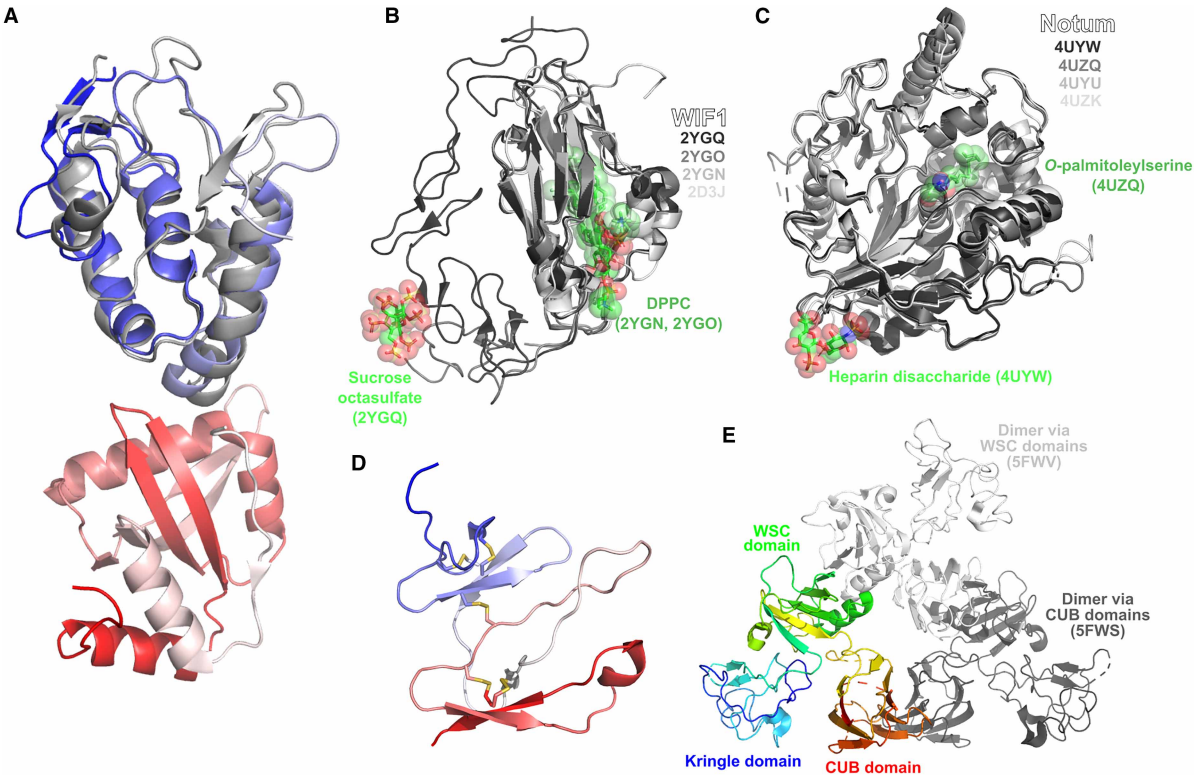

Figure 3. Structures related to interactions involving secreted negative regulators of Wnt signalling.
(**A**) Secreted Frizzled-related proteins. Legend: grey — mouse sFRP3 cysteine-rich domain (PDB 1IJX); blue-white-red N-to-C-terminal — *Xenopus* Sizzled (PDB 5XGP). (**B**) Wnt Inhibitory Factors (WIFs). Structures depicted include: NMR structure of WIF domain of native human WIF1 (PDB 2D3J); WIF domain of human WIF1 bound to dipalmitoylphosphatidylcholine (DPPC) (PDB 2YGN); WIF domain and epidermal growth factor-like (EGF-like) domain 1 of human WIF1 (PDB 2YGO); WIF domain and EGF-like domains 1–3 of human WIF bound to DPPC and sucrose octasulfate (PDB 2YGQ). (**C**) Notum. Structures depicted include: native *Drosophila* Notum (PDB 4UZK); native human Notum (PDB 4UYU); human Notum bound to *O*-palmitoleylserine (PDB 4UZQ); human Notum bound to heparin disaccharide (ΔUA(2S)α1-4GlcNS(6S) (PDB 4UYW). (**D**) NMR structure of mouse Dickkopf-2 (PDB 2JTK). Structure coloured from N-to-C-terminal by blue-white-red gradient. (**E**) Dimer formation by Kremen1. Monomeric Kremen1 (PDB 5FWU) is depicted as red-to-blue N-to-C terminal rainbow, with positions of second molecule in dimeric Kremen1 forms (PDB 5FWV, 5FWS) show as white/grey relative to monomeric form.

Kremens

In conjunction with DKKs, Kremens facilitate blocking of canonical Wnt signalling by promoting the endocytosis of LRPs. The structure of the Kremen1 ectodomain revealed a triangular arrangement of its Kringle, WSC and CUB domains [50] (Figure 3E). The Kringle and WSC domains bind DKK at the opposite face to its LRP-binding interface, while the CUB domain mediates Kremen1 dimerisation in a structure obtained from one of the crystal forms [50]. The WSC domain can also mediate dimerisation (Figure 3E).

Structure knowledge of Wnt receptors and co-receptors

Frizzleds (Fzds)

Together with the related Smoothened receptor, which mediates Hedgehog signalling, the Frizzleds form a class of G protein-coupled receptors that feature a seven-helical transmembrane domain (as per other GPCRs) and a distinctive cysteine-rich ectodomain (CRD) used to bind ligands. The structures of the CRDs of Fzd2 [51], Fzd4 [30,31,52,53], Fzd5 [54,55], Fzd7 [52,54–56] and Fzd8 [41,52,57] are presently represented in the Protein Data Bank; only a single Fzd transmembrane domain structure, that of Fzd4 [58], is presently known (Figure 4A,B). No structures featuring both the CRD and TM regions of Fzds are presently available. However,

Biochemical Society Transactions (2020) **48** 1765–1780
https://doi.org/10.1042/BST20200243

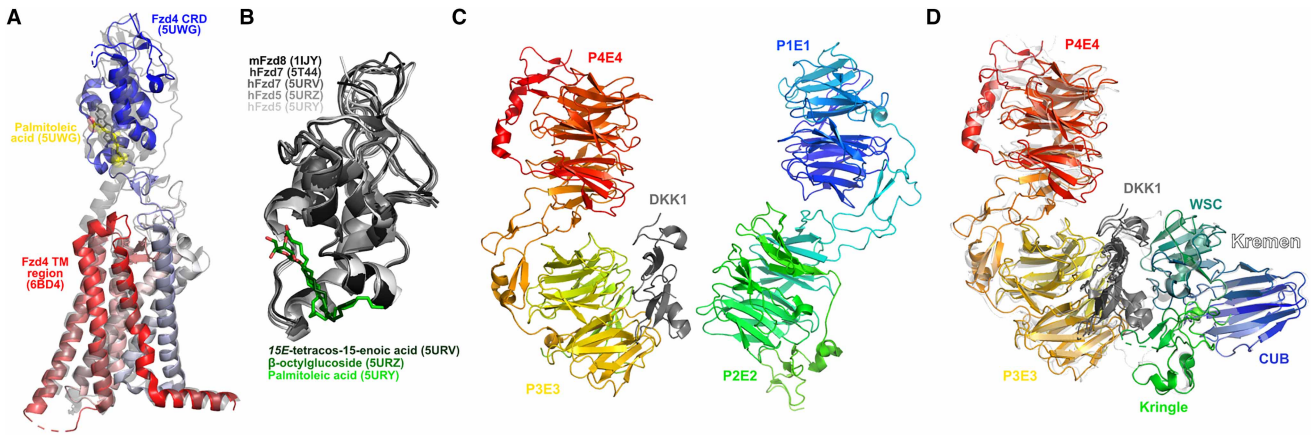

Figure 4. Structures related to transmembrane proteins.

(**A**) Frizzled-4 model generated by overlay of Frizzled-4 cysteine-rich domain (CRD) bound to palmitoleic acid (PDB 5UWG) and Frizzled-4 transmembrane (TM) region (PDB 6BD4) to Smoothened bound to cholesterol (PDB 5L7D; transparent grey). (**B**) Representative Frizzled CRD structures and complexes. Structures depicted include: native mouse Fzd8 CRD (PDB 1IJY), native human Fzd7 (PDB 5T44), human Fzd7 bound to *15E*-tetracos-15-enoic acid (PDB 5URV), human Fzd5 bound to β-octylglucoside (PDB 5URZ), human Fzd5 bound to palmitoleic acid (PDB 5URY). (**C**) Atomic structure of LRP6 ectodomain constructed from fitting X-ray structures of P1E1 and P2E2 regions (PDB 4DG6) and the complex of DKK1 with P3E3 and P4E4 regions (PDB 3S2K) to the electron microscopy structure (PDB 5GJE). Legend: red-to-blue rainbow — LRP6 N-to-C-terminal; grey — DKK1. (**D**) LRP6–DKK-Kremen interactions. LRP6–DKK1–Kremen1 complex (PDB 5FWW) depicted in colours; LRP6–DKK1 complex (PDB 3S2K), unbound DKK1 (PDB 2JTK) and unbound Kremen1 (PDB 5FWT) overlaid to PDB 5FWW and depicted in transparent grey.

the structural biology of the Fzds can be inferred from that of the more extensively structurally characterised Smoothened [59–66]. Of particular note is the recent determination of Smoothened in an active conformation bound to a G protein, revealing a similar opening of the intracellular regions of the receptor to that observed in other classes of GPCRs; such opening was earlier inferred to occurred in Fzds [67].

Low-density lipoprotein receptor-related proteins 5 and 6 (LRP5/6)

LRP5 and LRP6 function as Wnt ligand co-receptors in canonical Wnt signalling, and are antagonised by DKKs and Kremens. The ectodomain of LRP6 has been extensively structurally characterised and is primarily defined by the presence of four 7-bladed β-propellers followed by EGF-like domains (P1E1, P2E2, P3E3, P4E4) (Figure 4C). The structure of the combination of the LRP6 P1E1 and P2E2 regions [68], as well as that of the P3E3 and P4E4 regions [68–70], have been determined by X-ray crystallography, while the structure of the complete ectodomain has been determined by electron microscopy [69,71]. DKK1 has been structurally demonstrated to bind at the P1E1 [72] and P3E3 [50,68,70] regions, with Kremen binding on the opposite face of DKK to LRP, allowing formation of a ternary complex (Figure 4D).

Structural knowledge of intracellular proteins and complexes mediating Wnt signalling

Dishevelleds (Dvls)

Dvls feature three ordered domains: an N-terminal DIX domain, promoting Dvl oligomerisation into signalosomes, as well as mediating Axin binding; a PDZ domain, facilitating interactions with various proteins as well as weakly contributing to Fzd binding (although demonstrated to be dispensable for canonical Wnt signalling [73]); and a DEP domain, facilitating high affinity interaction with Fzds [74], as well as Fzd endocytosis [75]. These domains of Dvl1 and Dvl2 have been the focus of all currently published structures.

Structural characterisation of wildtype and mutant DIX domains of human Dvl2, mouse Dvl1 and mouse Dvl2 reveal in all instances the formation of a superhelical oligomeric structure [76–79]; the pitch of the superhelix varies appears to vary according to the specific DIX domain being examined, as well as through the introduction of interface mutants (Figure 5A). The variety of Dvl PDZ structures determined illustrate the flexibility of the domain's binding pocket to accommodate various ligands (Figure 5B) [80–83]. In particular, a series of structures

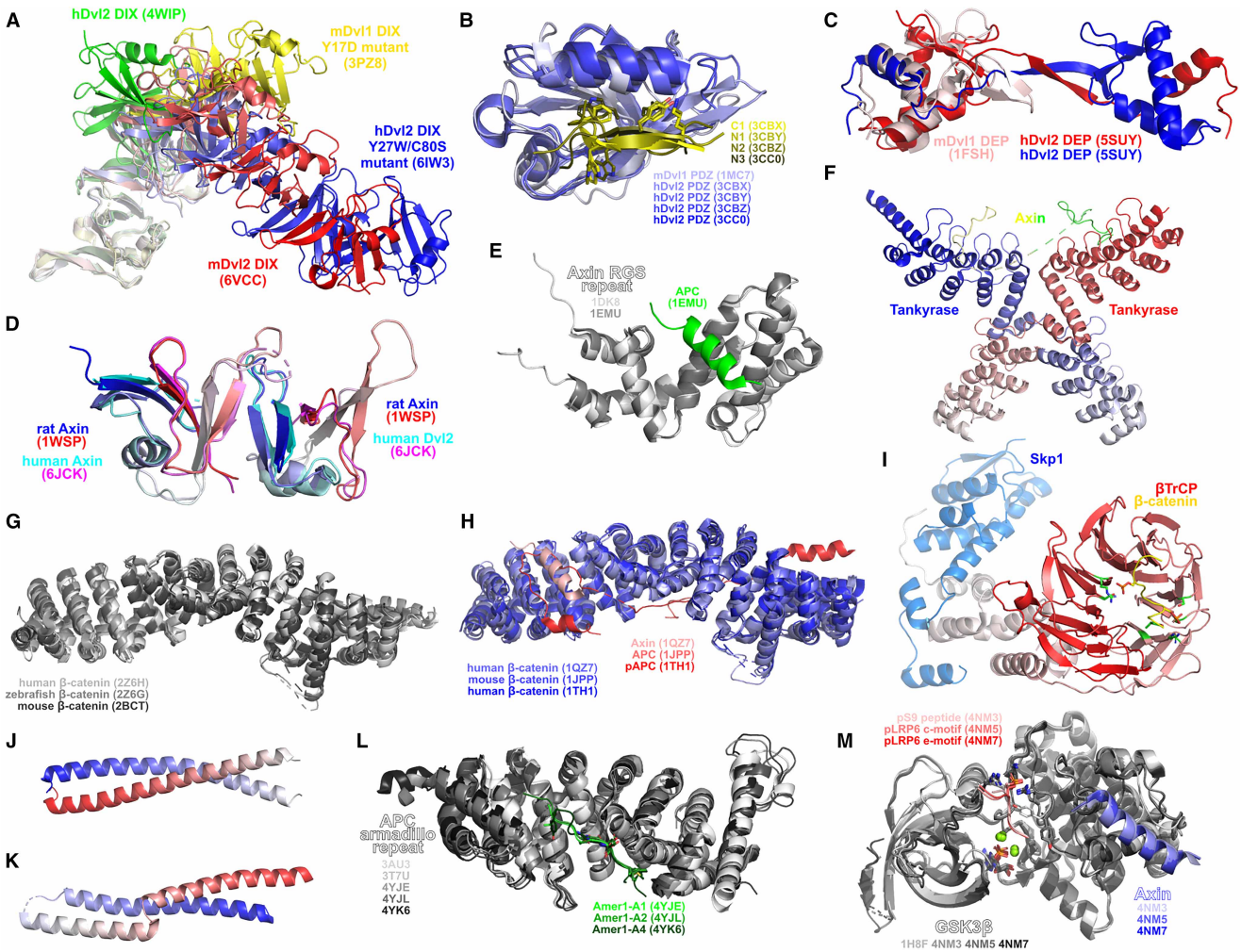

Figure 5. Structures related to cytoplasmic proteins and interactions.

(**A**) Dvl DIX domain oligomeric structures. (**B**) Dvl PDZ domain. Structures represented include: native mouse Dvl1 PDZ (PDB 1MC7), human Dvl2 PDZ in complex with C1 inhibitory peptide (PDB 3CBX), human Dvl2 PDZ in complex with N1 inhibitory peptide (PDB 3CBY), human Dvl2 PDZ in complex with N2 inhibitory peptide (PDB 3CBZ), human Dvl2 PDZ in complex with N3 inhibitory peptide (PDB 3CC0). The structure of the N2 complex with Dvl2 PDZ was inferred via the generation of a symmetry-related dimer. Selected residues with similar chemical functionality across multiple peptides — loosely highlighting how Fzd KTxxxW motifs may be recognised by Dvl PDZ domains — are shown as sticks. (**C**) Dvl DEP domain. Structures represented include: native mouse Dvl1 DEP domain (PDB 1FSH); human Dvl2 DEP domain dimer crystallised from dimeric fraction (PDB 5SUY). (**D**) Axin DIX domain. Structures represented include: rat Axin homodimer (PDB 1WSP); human Axin-Dvl2 heterodimer (PDB 6JCK). Each molecule coloured from N-to-C-terminal in blue-to-red/cyan-to-magenta gradient. (**E**) Axin RGS repeat in unbound (PDB 1DKS) and APC-bound (PDB 1EMU) states. (**F**) Mouse tankyrase-axin complex (PDB 3UTM). Each tankyrase monomer is coloured from N-to-C terminal as blue/red to white gradient. Dashes indicate missing portions of the axin structure. (**G**) Native β-catenin structures. (**H**) Complexes of interactions of cytoplasmic β-catenin. Structures represented include: human β-catenin bound to *Xenopus* Axin (PDB 1QZ7); mouse β-catenin bound to an APC fragment (PDB 1JPP); human β-catenin bound to a phosphorylated human APC fragment (PDB 1TH1). (**I**) APC N-terminal coiled-coil region (residues 2–55) (PDB 1DEB). Each chain coloured from N-to-C terminal as blue/red to white gradient. (**J**) APC N-terminal helical region (residues 126–250) (PDB 1M51). Coloured from N-to-C terminal as blue-white-red gradient. (**K**) APC armadillo repeat. Structures represented include: native APC (PDB 3AU3 and 3T7U); APC in complex with Amer1-A1 (PDB 4YJE); APC in complex with Amer1-A2 (PDB 4YJL); APC in complex with Amer1-A4 (PDB 4YK6). (**L**) β-TrCP-Skp1-β-catenin complex (PDB 1P22). Phosphate-contacting residues in β-TrCP are shown green. Phosphorylated β-catenin residues and their contacts in β-TrCP shown as sticks. (**M**) GSK3β complexes elaborating Wnt signalling. Structures represented include: *apo*-GSK3β (PDB 1H8F); GSK3β bound to N-terminal autoinhibitory phosphopeptide (pS9) and Axin (PDB 4NM3); GSK3β bound to phosphorylated LRP6 c-motif and Axin (PDB 4NM5); GSK3β bound to phosphorylated LRP6 e-motif and Axin (PDB 4NM7). Bound ADP, phosphorylated residues on peptides and Arg96, Arg180, Lys205 and Tyr216 shown as sticks. Magnesium shown as green spheres.

Biochemical Society Transactions (2020) **48** 1765–1780
https://doi.org/10.1042/BST20200243

of the human Dvl2 PDZ in complex with several peptides derived from phage display suggests how Dvl PDZ domains may recognise the C-terminal KTxxxW motifs contained in Fzds [81]. The structure of the mouse Dvl1 DEP domain was the first of any Dvl domain to be solved, demonstrating a fold exhibiting a strong electric dipole suggested to facilitate membrane targeting [84]. While the Dvl DEP domain has been illustrated to afford a key role in directly binding Fzds [74], the most recent structural evidence for any Dvl DEP domain — that of the human Dvl2 in a domain-swapped dimeric configuration — illustrate a potential role for the DEP domain in assembling Wnt signalosomes, as well as in mediating signal directionality [85] (Figure 5C).

Axin and tankyrase

Axin, like Dvl, contains a DIX domain which can undergo head-to-tail oligomerisation (Figure 5D). Recently, a complex between the Axin DIX domain and the Dvl2 DIX domain has been determined [86], revealing a similar structure of the Axin-Dvl heterodimer compared with both the Axin DIX homodimer [87] and Dvl homomer structures [76–79]. Although extended heterooligomer structures have not been demonstrated, these are presumed to form a superhelical structure with a varied pitch compared to the currently determined Dvl DIX homooligomer structures. Axin also directly interacts and has been structurally characterised with APC [88], GSK3β [89], β-catenin [90] and tankyrase. With the exception of its interaction with APC (Figure 5E), Axin utilises short segments to interact with these proteins (Figure 5F,H,L). The complex of Axin with the tankyrase ankyrin repeat reveals that the N-terminal of Axin binds to tankyrase in a 1:2 fashion (Figure 5F) [91].

β-catenin

The structures of the armadillo repeat regions of human [92], mouse [93] and zebrafish [92] β-catenin have been characterised, revealing a relatively conserved and remarkably rigid structure (Figure 5G). Complexes of this region of β-catenin with APC [90,94,95] and axin [88,96,97] have also been determined (Figure 5H). Axin utilises a short helical fragment to bind to armadillo repeats 3 and 4 of β-catenin, while APC uses an extended region to interact with approximately the entire length of β-catenin. Although part of APC binds to β-catenin at an overlapping region to Axin, APC does not share Axin's helical secondary structure in this location, indicating β-catenin's ability to bind peptides distinct in sequence and structure. N-terminal phosphorylation of β-catenin facilitates its destruction, and complexes of the phosphorylated N-terminal of β-catenin with the SCF ubiquitin ligase β-TrCP-Skp1 have been determined. These indicate that the phosphorylated N-terminal of β-catenin interacts with β-TrCP at the opposite face of the β-propeller to Skp1, with pSer33 bound by the first and second blades of the β-propeller and pSer37 bound by the fifth blade (Figure 5I) [98,99].

Adenomatous polyposis coli protein (APC)

APC is a very large protein comprising, in simplest terms, an N-terminal leucine-rich region (residues 1–730) and a C-terminal serine-rich region (residues 731–2832). Short fragments from the C-terminal serine-rich region have been structurally demonstrated in complex with a range of proteins, including axin (Figure 5E), β-catenin (Figure 5H), the Src-homology 3 domain of DDEF1 [100], and the PDZ1 [101] and PDZ2 [102] domains of DLG1. The N-terminal leucine-rich region contains at least three helical regions that have been structurally characterised: an N-terminal dimeric coiled-coil domain (residues 2–55) [103] (Figure 5J), an helical region forming a monomeric coiled-coil (residues 126–250) [104] (Figure 5K) and a series of armadillo repeats (residues 453–767) [105–109]. The N-terminal dimeric coiled-coil is poorly stable in isolation, suggesting that the dimerisation motif may extend beyond the first 55 amino acids of APC, although it is unclear whether the monomeric coiled-coil that follows contributes to dimerisation. The APC armadillo repeat region has been structurally characterised with several fragments of Amer1 (Figure 5L). These structures reveal that Amer1 fragments use a relatively functionally conserved motif to bind APC, consisting of Ser/Thr/Tyr to bind armadillo repeats 4–6 and a small polar amino acid (Gly/Ser/Cys) followed immediately by a glycine and a negatively charged amino acid to bind repeats 2–4. Hydrophobic amino acids (typically a longer chain aliphatic amino acid followed by alanine) bind repeats 1–3.

Glycogen synthase kinase 3β (GSK3β)

While GSK3β has been extensively structurally characterised as part of many medicinal chemistry research programs, a small selection of structures provide specific insight into its role in modulating Wnt signalling (Figure 5M). X-ray crystal structures of GSK3β in complex with the minimal binding segment of Axin [89] illustrate that Axin utilises an α-helical segment to bind GSK3β. The structures of GSK3β bound to its

phosphorylated autoinhibitory peptide and phosphorylated LRP6 motifs illustrate the importance of conformational changes in regulating GSK3β function and how primed substrates are recognised by GSK3β [15]. Specifically, the loop from residues 89-95 moves from the open conformation observed in the unbound state [110] to clamp onto the peptide, the phosphorylated residue is bound by three positively charged residues — Arg96, Arg180 and Lys205 — and Tyr216 rotates to facilitate peptide access to the active site.

Structural knowledge of intranuclear proteins and complexes mediating Wnt signalling

Nuclear β-catenin

Structures of TCFs [111–114] and LEF-1 [115] in complex with β-catenin (Figure 6A) reveal that β-catenin wraps around the N-terminal of these proteins, utilising approximately the full length of the armadillo repeats to bind the transcription factors, similar to how APC is bound by β-catenin (Figure 5H). Bcl9 binds to the first armadillo repeat of β-catenin using a short helix located between proline-rich stretches of its sequence, while the β-catenin inhibitor ICAT uses a small N-terminal helical domain to bind the final armadillo repeats of

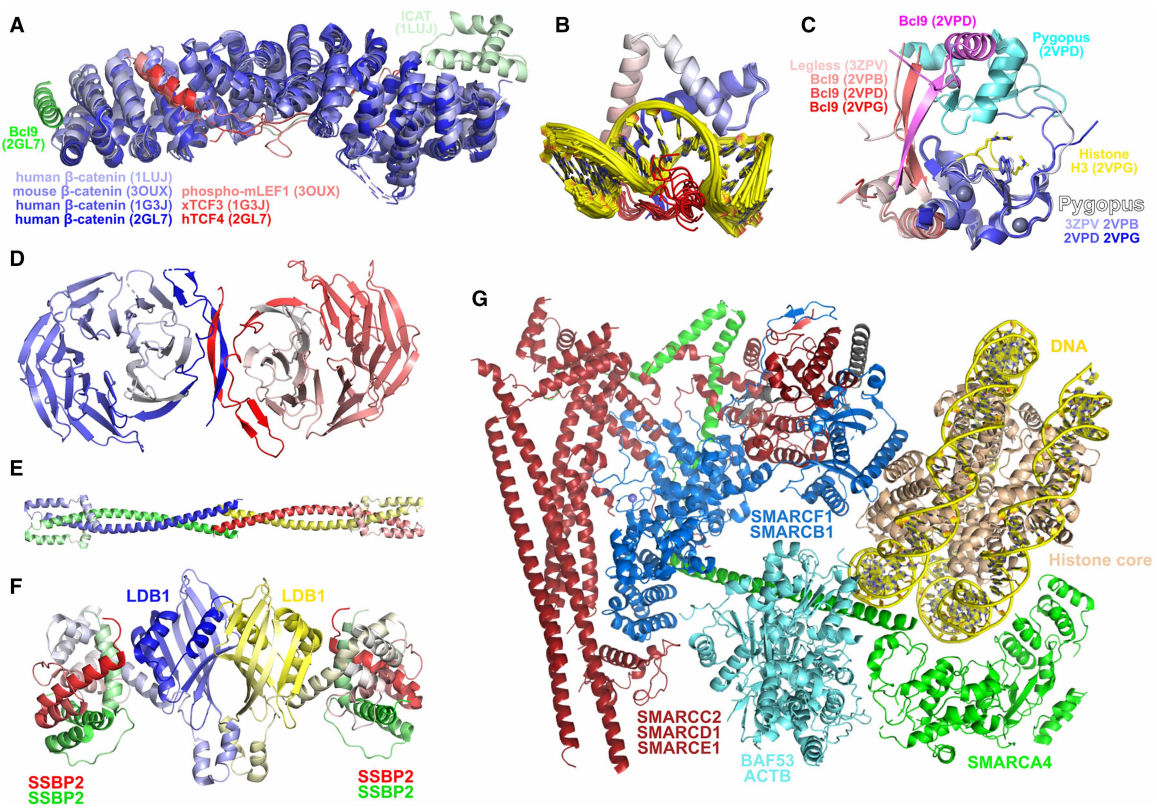

Figure 6. Structures related to intranuclear proteins and interactions.

(**A**) Nuclear β-catenin interactions. Structures represented include: human β-catenin bound to mouse ICAT (PDB 1LUJ), mouse β-catenin bound to phosphorylated mouse LEF1 (PDB 3OUX), human β-catenin bound to *Xenopus* TCF3 (PDB 1G3J), ternary complex of human β-catenin, human TCF4 and human Bcl9 (PDB 2GL7). (**B**) Mouse LEF1 high mobility group domain (blue–red N-to-C-terminal) bound to DNA (yellow) (PDB 2LEF). (**C**) Pygopus–Bcl9 interactions. Structure represented include: *Drosophila* Pygopus–Legless complex (PDB 3ZPV), human Pygopus1–Bcl9 complex (PDB 2VPB), human Pygopus1–Bcl9 dimer of dimers (PDB 2VPD), human Pygopus1–Bcl9-histone H3 tail ternary complex (PDB 2VPG). (**D**) TLE1 WD repeat dimer (PDB 1GXR). Legend: blue-white — molecule 1 N-to-C terminal; red-white — molecule 2 N-to-C terminal. (**E**) TLE1 Q domain tetramer (PDB 4OM2). Each chain coloured from N-to-C terminal in blue/red/yellow/green to white. (**F**) Assembly of the ChiLS complex in 4:2 stoichiometry based on available structures (PDB 6TYD and PDB 6S9S). (**G**) Structure of nucleosome-bound human BAF complex (PDB 6LTJ).

Biochemical Society Transactions (2020) **48** 1765–1780
https://doi.org/10.1042/BST20200243

β-catenin, and a C-terminal extension that overlaps with much of the TCF/LEF binding site, thus blocking TCF/LEF binding [97,116]. TCFs and LEFs utilise a high mobility group (HMG) box domain to bind DNA; the structure of the mouse LEF-1 HMG box domain bound to DNA was one of the earliest structures of such a domain, as well as a DNA–HMG box complex, and illustrates the bending of the DNA double helix characteristic of DNA–HMG box interactions (Figure 6B) [117].

B-cell CLL/lymphoma 9 protein (Bcl9) and Pygopus

Bcl9 forms a ternary complex with β-catenin and TCF transcription factors, binding at a distinct site on β-catenin to TCF, as well as other β-catenin-interacting proteins [111,118]. The function of Bcl9 is enhanced via binding to Pygopus proteins and their homologues, wherein a helical segment of Bcl9 interacts with the PHD-type zinc finger of Pygopus [119,120]; the Bcl9-like protein (BCL9L) forms a similar complex with Pygopus [121,122]. The human Bcl9–Pygopus heterodimer has been characterised in complex with a methylated histone fragment, illustrating the importance of Trp366 in Pygopus in interacting with methylated arginine and lysine; this residue is substituted for a phenylalanine in *Drosophila* Pygopus and likely facilitates similar interactions. Additionally, Bcl9 and Pygopus have been demonstrated to form a dimer of heterodimers; such an arrangement appears compatible with the binding of methylated histones (Figure 6C).

Groucho family proteins

Structures of the human Groucho family protein TLE1 have been obtained for its C-terminal WD repeat region, a seven-bladed β-propeller forming a dimer mediated by its N-terminal segment [123,124] (Figure 6D). The N-terminal Q domain, which mediates TCF binding, forms a dimeric coiled coil which in turn dimerises in a head-to-head fashion to give the active tetrameric species [125] (Figure 6E).

ChiLS complex

The biological assembly of the LUFS domain of the human SSDP2 revealed a tightly packed tetramer formed by dimerisation of dimers [126]. The biological assembly of the *Xenopus* LDB1 bound to darpin 10 illustrates the dimerisation of LDB proteins [21]. The biological assembly of the human SSDP2 in complex with the human LDB1 illustrates a 2:1 stoichiometry between SSDP2 and LDB1, with LDB1 binding at the tetramerization interface of SSDP2 [127]; this in turn suggests that the SSDP2 tetramer previously determined may represent an inactive state. Judicious overlay of the presently determined structures allows the development of a structural model of the ChiLS complex, displaying the determined 4 : 2 stoichiometry between the SSDP and LDB components [21] (Figure 6F).

BAF complex

The BAF complex is a very large complex comprised of numerous subunits that functions as a Wnt transcriptional co-activator. The SWI/SNF-related matrix-associated actin-dependent regulator of chromatin (SMARC) subfamily members, which are key components of this complex, have been the subject of numerous structural biology [128–130] and medicinal chemistry [131–133] efforts. Very recently, the structure of a nucleosome-bound human BAF complex has been determined [134] (Figure 6G). This structure reveals that SMARCC2 forms a dimeric coiled-coil, with which helical regions of SMARCD1 and SMARCE1 interact and which likely forms a scaffold for the complex. SMARCF1 contains an armadillo repeat-like region that interacts with this helical scaffold on one face and with the N-terminal domain of SMARCB1 with its opposing face. The SMARCB1 C-terminal domains interact with the SWIRM domains of both SMARCC1 molecules, an interaction that appears further stabilised by BAF45D. This assembly positions SMARCB1 to interact directly with histones H2A and H2B on one face of the nucleosome. SMARCA4 adopts a highly extended conformation, interacting with almost all subunits of the complex, cradling the opposite face of the nucleosome to SMARCB1 with its helicase domains. The extended conformation and nucleosome-binding by SMARCA4 appear to be supported through interaction with actin-like protein 6A (BAF53) and cytoplasmic actin 1 (ACTB).

Future challenges in the structural biology of Wnt signalling

Wnt structural biology has considerably grown in the past 20 years, however, there are still a number of notable gaps in knowledge. These include the structure of an active Wnt signalosome and/or components thereof (e.g. full length Fzd, Fzd in an active conformation, Fzd bound to Dvl), an overall view of the Wnt degradosome, and a comprehensive understanding of the structure of the Wnt enhanceosome. Cryoelectron

microscopy, which has facilitated the structural determination of many targets that were typically challenging or thought impossible by X-ray crystallography (including very large protein complexes and membrane-bound proteins in various states), has the potential to fill these gaps in structural knowledge of Wnt signalling. Nonetheless, significant protein engineering is likely to be required to achieve constructs sufficiently stable for structure determination, as has facilitated the elaboration of membrane protein structure and pharmacology. Computational approaches may also be valuable to fill some of these gaps — in particular, the combinatorial range of potential protein–protein interactions regulating the earlier stages of the pathway. The present structural data on canonical Wnt signalling affords numerous opportunities for structure-based drug design, with the recent growth allowing further dissection and effective targeting of this fascinating pathway.

Perspectives

- Canonical/β-catenin-dependent Wnt signalling is a pathway of enormous interest as a potential target in cancer treatment, as well as being crucial in the early stages of development.
- Structural knowledge of proteins and interactions involved in facilitating and antagonising canonical Wnt signalling has grown considerably over the past 20 years.
- Major frontiers to conquer relate primarily to understanding the assembly of large multiprotein complexes mediating Wnt signalling — in particular, the structure, activation and interactions of membrane receptors, as well as the assembly of nuclear proteins.

Competing Interests
The authors declare that there are no competing interests associated with the manuscript.

Funding
M.A. is a recipient of a Curtin Research Fellowship. S.Ö-G.P. is a recipient of an Institute of Genetics and Molecular Medicine Early Career Award.

Open Access
Open access for this article was enabled by the participation of University of Edinburgh in an all-inclusive *Read & Publish* pilot with Portland Press and the Biochemical Society under a transformative agreement with JISC.

Author Contribution
M.A. conceived the topic, identified relevant structures, prepared molecular structural figures and accompanying text. S.Ö-G.P. prepared the figure and text describing signalling background. Both authors critically reviewed and revised the manuscript.

Acknowledgements
Molecular structures presented in this work were identified by surveying UniProt and the Protein Data Bank for relevant proteins. All molecular structure figures were prepared using open-source PyMOL.

Abbreviations
APC, Adenomatous Polyposis Coli; BCL9, B-cell CLL/lymphoma 9 protein; ChiLS, Chip-SSDP/LIM-domain binding protein; CK1α, Casein kinase 1α; CRD, Cysteine-rich domain; CUB, Complement C1r/C1s, Uegf, Bmp1; Dkk, Dickkopf proteins; Dvl, Dishevelled; Fzd, Frizzled receptor; GSK3β, Glycogen synthase kinase 3β; HMG, High mobility group; LGR, Leucine-rich repeat-containing G-protein coupled receptor; LRP, low-density lipoprotein receptor; LRR, leucine-rich repeat; NLD, Netrin-like domain; PP2A, Protein phosphatase 2A; RSPO, R-spondin; SCF, Skp-Cullin-F-box; sFRP, secreted-Frizzled related protein; SMARC, SWI/SNF-related

Biochemical Society Transactions (2020) **48** 1765–1780
https://doi.org/10.1042/BST20200243

matrix-associated actin-dependent regulator of chromatin; TCF/LEF, T-cell factor/lymphoid enhancer factor; WIF, Wnt inhibitory factor; WSC, Cell wall integrity and stress response components.

References

1 Olsen, J.J., Pohl, S.O., Deshmukh, A., Visweswaran, M., Ward, N.C., Arfuso, F. et al. (2017) The role of Wnt signalling in angiogenesis. *Clin. Biochem. Rev.* **38**, 131–142 PMID:29332977

2 Nusse, R. and Clevers, H. (2017) Wnt/beta-catenin signaling, disease, and emerging therapeutic modalities. *Cell* **169**, 985–999 https://doi.org/10.1016/j.cell.2017.05.016

3 Pohl, S.G., Brook, N., Agostino, M., Arfuso, F., Kumar, A.P. and Dharmarajan, A. (2017) Wnt signaling in triple-negative breast cancer. *Oncogenesis* **6**, e310 https://doi.org/10.1038/oncsis.2017.14

4 Clevers, H. and Nusse, R. (2012) Wnt/beta-catenin signaling and disease. *Cell* **149**, 1192–1205 https://doi.org/10.1016/j.cell.2012.05.012

5 Clevers, H., Loh, K.M. and Nusse, R. (2014) Stem cell signaling. An integral program for tissue renewal and regeneration: Wnt signaling and stem cell control. *Science* **346**, 1248012 https://doi.org/10.1126/science.1248012

6 Gammons, M. and Bienz, M. (2018) Multiprotein complexes governing Wnt signal transduction. *Curr. Opin. Cell Biol.* **51**, 42–49 https://doi.org/10.1016/j.ceb.2017.10.008

7 Lebensohn, A.M. and Rohatgi, R. (2018) R-spondins can potentiate WNT signaling without LGRs. *eLife.* **7**, e33126 https://doi.org/10.7554/eLife.33126

8 Hao, H.X., Xie, Y., Zhang, Y., Charlat, O., Oster, E., Avello, M. et al. (2012) ZNRF3 promotes Wnt receptor turnover in an R-spondin-sensitive manner. *Nature* **485**, 195–200 https://doi.org/10.1038/nature11019

9 Koo, B.K., Spit, M., Jordens, I., Low, T.Y., Stange, D.E., van de Wetering, M. et al. (2012) Tumour suppressor RNF43 is a stem-cell E3 ligase that induces endocytosis of Wnt receptors. *Nature* **488**, 665–669 https://doi.org/10.1038/nature11308

10 Ke, J., Harikumar, K.G., Erice, C., Chen, C., Gu, X., Wang, L. et al. (2013) Structure and function of Norrin in assembly and activation of a Frizzled 4-Lrp5/6 complex. *Genes Dev.* **27**, 2305–2319 https://doi.org/10.1101/gad.228544.113

11 Lai, M.B., Zhang, C., Shi, J., Johnson, V., Khandan, L., McVey, J. et al. (2017) TSPAN12 is a Norrin co-receptor that amplifies Frizzled4 ligand selectivity and signaling. *Cell Rep.* **19**, 2809–2822 https://doi.org/10.1016/j.celrep.2017.06.004

12 Carmon, K.S., Gong, X., Lin, Q., Thomas, A. and Liu, Q. (2011) R-spondins function as ligands of the orphan receptors LGR4 and LGR5 to regulate Wnt/beta-catenin signaling. *Proc. Natl Acad. Sci. U.S.A.* **108**, 11452–7 https://doi.org/10.1073/pnas.1106083108

13 Stamos, J.L. and Weis, W.I. (2013) The beta-catenin destruction complex. *Cold Spring Harb. Perspect. Biol.* **5**, a007898 https://doi.org/10.1101/cshperspect.a007898

14 Tanneberger, K., Pfister, A.S., Brauburger, K., Schneikert, J., Hadjihannas, M.V., Kriz, V. et al. (2011) Amer1/WTX couples Wnt-induced formation of PtdIns(4,5)P2 to LRP6 phosphorylation. *EMBO J.* **30**, 1433–1443 https://doi.org/10.1038/emboj.2011.28

15 Stamos, J.L., Chu, M.L., Enos, M.D., Shah, N. and Weis, W.I. (2014) Structural basis of GSK-3 inhibition by N-terminal phosphorylation and by the Wnt receptor LRP6. *eLife.* **3**, e01998 https://doi.org/10.7554/eLife.01998

16 Wu, G., Huang, H., Garcia Abreu, J. and He, X. (2009) Inhibition of GSK3 phosphorylation of beta-catenin via phosphorylated PPPSPXS motifs of Wnt coreceptor LRP6. *PLoS ONE* **4**, e4926 https://doi.org/10.1371/journal.pone.0004926

17 Piao, S., Lee, S.H., Kim, H., Yum, S., Stamos, J.L., Xu, Y. et al. (2008) Direct inhibition of GSK3beta by the phosphorylated cytoplasmic domain of LRP6 in Wnt/beta-catenin signaling. *PLoS ONE* **3**, e4046 https://doi.org/10.1371/journal.pone.0004046

18 Cselenyi, C.S., Jernigan, K.K., Tahinci, E., Thorne, C.A., Lee, L.A. and Lee, E. (2008) LRP6 transduces a canonical Wnt signal independently of Axin degradation by inhibiting GSK3's phosphorylation of beta-catenin. *Proc. Natl Acad. Sci. U.S.A.* **105**, 8032–8037 https://doi.org/10.1073/pnas.0803025105

19 Mariotti, L., Pollock, K. and Guettler, S. (2017) Regulation of Wnt/beta-catenin signalling by tankyrase-dependent poly(ADP-ribosyl)ation and scaffolding. *Br. J. Pharmacol.* **174**, 4611–4636 https://doi.org/10.1111/bph.14038

20 Fiedler, M., Graeb, M., Mieszczanek, J., Rutherford, T.J., Johnson, C.M. and Bienz, M. (2015) An ancient Pygo-dependent Wnt enhanceosome integrated by chip/LDB-SSDP. *eLife* **4**, e09073 https://doi.org/10.7554/eLife.09073

21 Renko, M., Fiedler, M., Rutherford, T.J., Schaefer, J.V., Pluckthun, A. and Bienz, M. (2019) Rotational symmetry of the structured Chip/LDB-SSDP core module of the Wnt enhanceosome. *Proc. Natl Acad. Sci. U.S.A.* **116**, 20977–20983 https://doi.org/10.1073/pnas.1912705116

22 van Tienen, L.M., Mieszczanek, J., Fiedler, M., Rutherford, T.J. and Bienz, M. (2017) Constitutive scaffolding of multiple Wnt enhanceosome components by Legless/BCL9. *eLife* **6**, e20882 https://doi.org/10.7554/eLife.20882

23 Janda, C.Y., Waghray, D., Levin, A.M., Thomas, C. and Garcia, K.C. (2012) Structural basis of Wnt recognition by Frizzled. *Science* **337**, 59–64 https://doi.org/10.1126/science.1222879

24 Hirai, H., Matoba, K., Mihara, E., Arimori, T. and Takagi, J. (2019) Crystal structure of a mammalian Wnt-frizzled complex. *Nat. Struct. Mol. Biol.* **26**, 372–379 https://doi.org/10.1038/s41594-019-0216-z

25 Agostino, M. and Pohl, S.O. (2019) Wnt binding affinity prediction for putative Frizzled-type cysteine-rich domains. *Int. J. Mol. Sci.* **20**, 4168 https://doi.org/10.3390/ijms20174168

26 Agostino, M., Pohl, S.O. and Dharmarajan, A. (2017) Structure-based prediction of Wnt binding affinities for Frizzled-type cysteine-rich domains. *J. Biol. Chem.* **292**, 11218–11229 https://doi.org/10.1074/jbc.M117.786269

27 Ain, Q.U., Seemab, U., Rashid, S., Nawaz, M.S. and Kamal, M.A. (2013) Prediction of structure of human WNT-CRD (FZD) complex for computational drug repurposing. *PLoS ONE* **8**, e54630 https://doi.org/10.1371/journal.pone.0054630

28 Chu, M.L., Ahn, V.E., Choi, H.J., Daniels, D.L., Nusse, R. and Weis, W.I. (2013) Structural studies of Wnts and identification of an LRP6 binding site. *Structure* **21**, 1235–1242 https://doi.org/10.1016/j.str.2013.05.006

29 Ching, W., Hang, H.C. and Nusse, R. (2008) Lipid-independent secretion of a Drosophila Wnt protein. *J. Biol. Chem.* **283**, 17092–8 https://doi.org/10.1074/jbc.M802059200

30 Shen, G., Ke, J., Wang, Z., Cheng, Z., Gu, X., Wei, Y. et al. (2015) Structural basis of the Norrin-Frizzled 4 interaction. *Cell Res.* **25**, 1078–1081 https://doi.org/10.1038/cr.2015.92

31 Chang, T.H., Hsieh, F.L., Zebisch, M., Harlos, K., Elegheert, J. and Jones, E.Y. (2015) Structure and functional properties of Norrin mimic Wnt for signalling with Frizzled4, Lrp5/6, and proteoglycan. *eLife* **4**, e06554 https://doi.org/10.7554/eLife.06554

32 Zebisch, M., Xu, Y., Krastev, C., MacDonald, B.T., Chen, M., Gilbert, R.J. et al. (2013) Structural and molecular basis of ZNRF3/RNF43 transmembrane ubiquitin ligase inhibition by the Wnt agonist R-spondin. *Nat. Commun.* **4**, 2787 https://doi.org/10.1038/ncomms3787
33 Peng, W.C., de Lau, W., Forneris, F., Granneman, J.C., Huch, M., Clevers, H. et al. (2013) Structure of stem cell growth factor R-spondin 1 in complex with the ectodomain of its receptor LGR5. *Cell Rep.* **3**, 1885–1892 https://doi.org/10.1016/j.celrep.2013.06.009
34 Xu, K., Xu, Y., Rajashankar, K.R., Robev, D. and Nikolov, D.B. (2013) Crystal structures of Lgr4 and its complex with R-spondin1. *Structure* **21**, 1683–1689 https://doi.org/10.1016/j.str.2013.07.001
35 Wang, D., Huang, B., Zhang, S., Yu, X., Wu, W. and Wang, X. (2013) Structural basis for R-spondin recognition by LGR4/5/6 receptors. *Genes Dev.* **27**, 1339–1344 https://doi.org/10.1101/gad.219360.113
36 Zebisch, M. and Jones, E.Y. (2015) Crystal structure of R-spondin 2 in complex with the ectodomains of its receptors LGR5 and ZNRF3. *J. Struct. Biol.* **191**, 149–155 https://doi.org/10.1016/j.jsb.2015.05.008
37 Peng, W.C., de Lau, W., Madoori, P.K., Forneris, F., Granneman, J.C., Clevers, H. et al. (2013) Structures of Wnt-antagonist ZNRF3 and its complex with R-spondin 1 and implications for signaling. *PLoS ONE* **8**, e83110 https://doi.org/10.1371/journal.pone.0083110
38 Chen, P.H., Chen, X., Lin, Z., Fang, D. and He, X. (2013) The structural basis of R-spondin recognition by LGR5 and RNF43. *Genes Dev.* **27**, 1345–1350 https://doi.org/10.1101/gad.219915.113
39 Pohl, S., Scott, R., Arfuso, F., Perumal, V. and Dharmarajan, A. (2015) Secreted frizzled-related protein 4 and its implications in cancer and apoptosis. *Tumour Biol.* **36**, 143–152 https://doi.org/10.1007/s13277-014-2956-z
40 Bovolenta, P., Esteve, P., Ruiz, J.M., Cisneros, E. and Lopez-Rios, J. (2008) Beyond Wnt inhibition: new functions of secreted Frizzled-related proteins in development and disease. *J. Cell Sci.* **121**, 737–746 https://doi.org/10.1242/jcs.026096
41 Dann, C.E., Hsieh, J.C., Rattner, A., Sharma, D., Nathans, J. and Leahy, D.J. (2001) Insights into Wnt binding and signalling from the structures of two Frizzled cysteine-rich domains. *Nature* **412**, 86–90 https://doi.org/10.1038/35083601
42 Bu, Q., Li, Z., Zhang, J., Xu, F., Liu, J. and Liu, H. (2017) The crystal structure of full-length sizzled from *Xenopus laevis* yields insights into Wnt-antagonistic function of secreted Frizzled-related proteins. *J. Biol. Chem.* **292**, 16055–16069 https://doi.org/10.1074/jbc.M117.791756
43 Poggi, L., Casarosa, S. and Carl, M. (2018) An eye on the Wnt inhibitory factor Wif1. *Front. Cell Dev. Biol.* **6**, 167 https://doi.org/10.3389/fcell.2018.00167
44 Liepinsh, E., Banyai, L., Patthy, L. and Otting, G. (2006) NMR structure of the WIF domain of the human Wnt-inhibitory factor-1. *J. Mol. Biol.* **357**, 942–950 https://doi.org/10.1016/j.jmb.2006.01.047
45 Malinauskas, T., Aricescu, A.R., Lu, W., Siebold, C. and Jones, E.Y. (2011) Modular mechanism of Wnt signaling inhibition by Wnt inhibitory factor 1. *Nat. Struct. Mol. Biol.* **18**, 886–893 https://doi.org/10.1038/nsmb.2081
46 Kakugawa, S., Langton, P.F., Zebisch, M., Howell, S., Chang, T.H., Liu, Y. et al. (2015) Notum deacylates Wnt proteins to suppress signalling activity. *Nature* **519**, 187–192 https://doi.org/10.1038/nature14259
47 Bao, J., Zheng, J.J. and Wu, D. (2012) The structural basis of DKK-mediated inhibition of Wnt/LRP signaling. *Sci. Signal.* **5**, pe22 https://doi.org/10.1126/scisignal.2003028
48 Mao, B., Wu, W., Davidson, G., Marhold, J., Li, M., Mechler, B.M. et al. (2002) Kremen proteins are Dickkopf receptors that regulate Wnt/beta-catenin signalling. *Nature* **417**, 664–667 https://doi.org/10.1038/nature756
49 Chen, L., Wang, K., Shao, Y., Huang, J., Li, X., Shan, J. et al. (2008) Structural insight into the mechanisms of Wnt signaling antagonism by Dkk. *J. Biol. Chem.* **283**, 23364–23370 https://doi.org/10.1074/jbc.M802375200
50 Zebisch, M., Jackson, V.A., Zhao, Y. and Jones, E.Y. (2016) Structure of the dual-mode Wnt regulator Kremen1 and insight into ternary complex formation with LRP6 and Dickkopf. *Structure* **24**, 1599–1605 https://doi.org/10.1016/j.str.2016.06.020
51 Chen, P., Tao, L., Wang, T., Zhang, J., He, A., Lam, K.H. et al. (2018) Structural basis for recognition of frizzled proteins by Clostridium difficile toxin B. *Science* **360**, 664–669 https://doi.org/10.1126/science.aar1999
52 Dang, L.T., Miao, Y., Ha, A., Yuki, K., Park, K., Janda, C.Y. et al. (2019) Receptor subtype discrimination using extensive shape complementary designed interfaces. *Nat. Struct. Mol. Biol.* **26**, 407–414 https://doi.org/10.1038/s41594-019-0224-z
53 DeBruine, Z.J., Ke, J., Harikumar, K.G., Gu, X., Borowsky, P., Williams, B.O. et al. (2017) Wnt5a promotes Frizzled-4 signalosome assembly by stabilizing cysteine-rich domain dimerization. *Genes Dev.* **31**, 916–926 https://doi.org/10.1101/gad.298331.117
54 Nile, A.H., Mukund, S., Stanger, K., Wang, W. and Hannoush, R.N. (2017) Unsaturated fatty acyl recognition by Frizzled receptors mediates dimerization upon Wnt ligand binding. *Proc. Natl Acad. Sci. U.S.A.* **114**, 4147–4152 https://doi.org/10.1073/pnas.1618293114
55 Raman, S., Beilschmidt, M., To, M., Lin, K., Lui, F., Jmeian, Y. et al. (2019) Structure-guided design fine-tunes pharmacokinetics, tolerability, and antitumor profile of multispecific frizzled antibodies. *Proc. Natl Acad. Sci. U.S.A.* **116**, 6812–6817 https://doi.org/10.1073/pnas.1817246116
56 Nile, A.H., de Sousa, E.M.F., Mukund, S., Piskol, R., Hansen, S., Zhou, L. et al. (2018) A selective peptide inhibitor of Frizzled 7 receptors disrupts intestinal stem cells. *Nat. Chem. Biol.* **14**, 582–590 https://doi.org/10.1038/s41589-018-0035-2
57 Janda, C.Y., Dang, L.T., You, C., Chang, J., de Lau, W., Zhong, Z.A. et al. (2017) Surrogate Wnt agonists that phenocopy canonical Wnt and beta-catenin signalling. *Nature* **545**, 234–237 https://doi.org/10.1038/nature22306
58 Yang, S., Wu, Y., Xu, T.H., de Waal, P.W., He, Y., Pu, M. et al. (2018) Crystal structure of the Frizzled 4 receptor in a ligand-free state. *Nature* **560**, 666–670 https://doi.org/10.1038/s41586-018-0447-x
59 Byrne, E.F.X., Sircar, R., Miller, P.S., Hedger, G., Luchetti, G., Nachtergaele, S. et al. (2016) Structural basis of smoothened regulation by its extracellular domains. *Nature* **535**, 517–522 https://doi.org/10.1038/nature18934
60 Deshpande, I., Liang, J., Hedeen, D., Roberts, K.J., Zhang, Y., Ha, B. et al. (2019) Smoothened stimulation by membrane sterols drives Hedgehog pathway activity. *Nature* **571**, 284–288 https://doi.org/10.1038/s41586-019-1355-4
61 Hedger, G., Koldso, H., Chavent, M., Siebold, C., Rohatgi, R. and Sansom, M.S.P. (2019) Cholesterol interaction sites on the transmembrane domain of the hedgehog signal transducer and class F G protein-coupled receptor smoothened. *Structure* **27**, 549–559 https://doi.org/10.1016/j.str.2018.11.003
62 Huang, P., Nedelcu, D., Watanabe, M., Jao, C., Kim, Y., Liu, J. et al. (2016) Cellular cholesterol directly activates smoothened in hedgehog signaling. *Cell* **166**, 1176–1187 https://doi.org/10.1016/j.cell.2016.08.003
63 Qi, X., Liu, H., Thompson, B., McDonald, J., Zhang, C. and Li, X. (2019) Cryo-EM structure of oxysterol-bound human smoothened coupled to a heterotrimeric Gi. *Nature* **571**, 279–283 https://doi.org/10.1038/s41586-019-1286-0

64 Wang, C., Wu, H., Evron, T., Vardy, E., Han, G.W., Huang, X.P. et al. (2014) Structural basis for smoothened receptor modulation and chemoresistance to anticancer drugs. *Nat. Commun.* **5**, 4355 https://doi.org/10.1038/ncomms5355
65 Wang, C., Wu, H., Katritch, V., Han, G.W., Huang, X.P., Liu, W. et al. (2013) Structure of the human smoothened receptor bound to an antitumour agent. *Nature* **497**, 338–343 https://doi.org/10.1038/nature12167
66 Zhang, X., Zhao, F., Wu, Y., Yang, J., Han, G.W., Zhao, S. et al. (2017) Crystal structure of a multi-domain human smoothened receptor in complex with a super stabilizing ligand. *Nat. Commun.* **8**, 15383 https://doi.org/10.1038/ncomms15383
67 Wright, S.C., Cañizal, M.C.A., Benkel, T., Simon, K., Le Gouill, C., Matricon, P. et al. (2018) FZD5 is a Gαq-coupled receptor that exhibits the functional hallmarks of prototypical GPCRs. *Sci. Signal.* **11**, eaar5536 https://doi.org/10.1126/scisignal.aar5536
68 Cheng, Z., Biechele, T., Wei, Z., Morrone, S., Moon, R.T., Wang, L. et al. (2011) Crystal structures of the extracellular domain of LRP6 and its complex with DKK1. *Nat. Struct. Mol. Biol.* **18**, 1204–1210 https://doi.org/10.1038/nsmb.2139
69 Chen, S., Bubeck, D., MacDonald, B.T., Liang, W.X., Mao, J.H., Malinauskas, T. et al. (2011) Structural and functional studies of LRP6 ectodomain reveal a platform for Wnt signaling. *Dev. Cell* **21**, 848–861 https://doi.org/10.1016/j.devcel.2011.09.007
70 Ahn, V.E., Chu, M.L., Choi, H.J., Tran, D., Abo, A. and Weis, W.I. (2011) Structural basis of Wnt signaling inhibition by Dickkopf binding to LRP5/6. *Dev. Cell* **21**, 862–873 https://doi.org/10.1016/j.devcel.2011.09.003
71 Matoba, K., Mihara, E., Tamura-Kawakami, K., Miyazaki, N., Maeda, S., Hirai, H. et al. (2017) Conformational freedom of the LRP6 ectodomain is regulated by N-glycosylation and the binding of the Wnt antagonist Dkk1. *Cell Rep.* **18**, 32–40 https://doi.org/10.1016/j.celrep.2016.12.017
72 Bourhis, E., Wang, W., Tam, C., Hwang, J., Zhang, Y., Spittler, D. et al. (2011) Wnt antagonists bind through a short peptide to the first beta-propeller domain of LRP5/6. *Structure* **19**, 1433–1442 https://doi.org/10.1016/j.str.2011.07.005
73 Gammons, M.V., Rutherford, T.J., Steinhart, Z., Angers, S. and Bienz, M. (2016) Essential role of the dishevelled DEP domain in a Wnt-dependent human-cell-based complementation assay. *J. Cell Sci.* **129**, 3892–3902 https://doi.org/10.1242/jcs.195685
74 Tauriello, D.V., Jordens, I., Kirchner, K., Slootstra, J.W., Kruitwagen, T., Bouwman, B.A. et al. (2012) Wnt/beta-catenin signaling requires interaction of the dishevelled DEP domain and C terminus with a discontinuous motif in Frizzled. *Proc. Natl Acad. Sci. U.S.A.* **109**, E812–E820 https://doi.org/10.1073/pnas.1114802109
75 Yu, A., Xing, Y., Harrison, S.C. and Kirchhausen, T. (2010) Structural analysis of the interaction between Dishevelled2 and clathrin AP-2 adaptor, a critical step in noncanonical Wnt signaling. *Structure* **18**, 1311–1320 https://doi.org/10.1016/j.str.2010.07.010
76 Kan, W., Enos, M.D., Korkmazhan, E., Muennich, S., Chen, D.H., Gammons, M.V. et al. (2020) Limited dishevelled/Axin oligomerization determines efficiency of Wnt/beta-catenin signal transduction. *eLife* **9**, e55015 https://doi.org/10.7554/eLife.55015
77 Yamanishi, K., Sin, Y., Terawaki, S.I., Higuchi, Y. and Shibata, N. (2019) High-resolution structure of a Y27W mutant of the Dishevelled2 DIX domain. *Acta Crystallogr. F Struct. Biol. Commun.* **75**, 116–122 https://doi.org/10.1107/S2053230X18018290
78 Madrzak, J., Fiedler, M., Johnson, C.M., Ewan, R., Knebel, A., Bienz, M. et al. (2015) Ubiquitination of the dishevelled DIX domain blocks its head-to-tail polymerization. *Nat. Commun.* **6**, 6718 https://doi.org/10.1038/ncomms7718
79 Liu, Y.T., Dan, Q.J., Wang, J., Feng, Y., Chen, L., Liang, J. et al. (2011) Molecular basis of Wnt activation via the DIX domain protein Ccd1. *J. Biol. Chem.* **286**, 8597–8608 https://doi.org/10.1074/jbc.M110.186742
80 Cheyette, B.N., Waxman, J.S., Miller, J.R., Takemaru, K., Sheldahl, L.C., Khlebtsova, N. et al. (2002) Dapper, a dishevelled-associated antagonist of beta-catenin and JNK signaling, is required for notochord formation. *Dev. Cell* **2**, 449–461 https://doi.org/10.1016/S1534-5807(02)00140-5
81 Zhang, Y., Appleton, B.A., Wiesmann, C., Lau, T., Costa, M., Hannoush, R.N. et al. (2009) Inhibition of Wnt signaling by dishevelled PDZ peptides. *Nat. Chem. Biol.* **5**, 217–219 https://doi.org/10.1038/nchembio.152
82 Wong, H.C., Bourdelas, A., Krauss, A., Lee, H.J., Shao, Y., Wu, D. et al. (2003) Direct binding of the PDZ domain of dishevelled to a conserved internal sequence in the C-terminal region of Frizzled. *Mol. Cell* **12**, 1251–1260 https://doi.org/10.1016/S1097-2765(03)00427-1
83 Lee, H.J., Wang, N.X., Shi, D.L. and Zheng, J.J. (2009) Sulindac inhibits canonical Wnt signaling by blocking the PDZ domain of the protein dishevelled. *Angew. Chem. Int. Ed. Engl.* **48**, 6448–6452 https://doi.org/10.1002/anie.200902981
84 Wong, H.C., Mao, J., Nguyen, J.T., Srinivas, S., Zhang, W., Liu, B. et al. (2000) Structural basis of the recognition of the dishevelled DEP domain in the Wnt signaling pathway. *Nat. Struct. Biol.* **7**, 1178–1184 https://doi.org/10.1038/82047
85 Gammons, M.V., Renko, M., Johnson, C.M., Rutherford, T.J. and Bienz, M. (2016) Wnt signalosome assembly by DEP domain swapping of dishevelled. *Mol. Cell* **64**, 92–104 https://doi.org/10.1016/j.molcel.2016.08.026
86 Yamanishi, K., Fiedler, M., Terawaki, S.I., Higuchi, Y., Bienz, M. and Shibata, N. (2019) A direct heterotypic interaction between the DIX domains of dishevelled and axin mediates signaling to beta-catenin. *Sci. Signal.* **12**, eaaw5505 https://doi.org/10.1126/scisignal.aaw5505
87 Schwarz-Romond, T., Fiedler, M., Shibata, N., Butler, P.J., Kikuchi, A., Higuchi, Y. et al. (2007) The DIX domain of dishevelled confers Wnt signaling by dynamic polymerization. *Nat. Struct. Mol. Biol.* **14**, 484–492 https://doi.org/10.1038/nsmb1247
88 Spink, K.E., Polakis, P. and Weis, W.I. (2000) Structural basis of the axin-adenomatous polyposis coli interaction. *EMBO J.* **19**, 2270–2279 https://doi.org/10.1093/emboj/19.10.2270
89 Dajani, R., Fraser, E., Roe, S.M., Yeo, M., Good, V.M., Thompson, V. et al. (2003) Structural basis for recruitment of glycogen synthase kinase 3beta to the axin-APC scaffold complex. *EMBO J.* **22**, 494–501 https://doi.org/10.1093/emboj/cdg068
90 Xing, Y., Clements, W.K., Le Trong, I., Hinds, T.R., Stenkamp, R., Kimelman, D. et al. (2004) Crystal structure of a beta-catenin/APC complex reveals a critical role for APC phosphorylation in APC function. *Mol. Cell* **15**, 523–533 https://doi.org/10.1016/j.molcel.2004.08.001
91 Morrone, S., Cheng, Z., Moon, R.T., Cong, F. and Xu, W. (2012) Crystal structure of a Tankyrase-Axin complex and its implications for axin turnover and Tankyrase substrate recruitment. *Proc. Natl Acad. Sci. U.S.A.* **109**, 1500–1505 https://doi.org/10.1073/pnas.1116618109
92 Xing, Y., Takemaru, K., Liu, J., Berndt, J.D., Zheng, J.J., Moon, R.T. et al. (2008) Crystal structure of a full-length beta-catenin. *Structure* **16**, 478–487 https://doi.org/10.1016/j.str.2007.12.021
93 Huber, A.H., Nelson, W.J. and Weis, W.I. (1997) Three-dimensional structure of the armadillo repeat region of beta-catenin. *Cell* **90**, 871–882 https://doi.org/10.1016/S0092-8674(00)80352-9
94 Ha, N.C., Tonozuka, T., Stamos, J.L., Choi, H.J. and Weis, W.I. (2004) Mechanism of phosphorylation-dependent binding of APC to beta-catenin and its role in beta-catenin degradation. *Mol. Cell* **15**, 511–521 https://doi.org/10.1016/j.molcel.2004.08.010

95 Spink K, E., Fridman, S.G. and Weis, W.I. (2001) Molecular mechanisms of beta-catenin recognition by adenomatous polyposis coli revealed by the structure of an APC-beta-catenin complex. *EMBO J.* **20**, 6203–6212 https://doi.org/10.1093/emboj/20.22.6203
96 Xing, Y., Clements, W.K., Kimelman, D. and Xu, W. (2003) Crystal structure of a beta-catenin/axin complex suggests a mechanism for the beta-catenin destruction complex. *Genes Dev.* **17**, 2753–2764 https://doi.org/10.1101/gad.1142603
97 Daniels, D.L. and Weis, W.I. (2002) ICAT inhibits beta-catenin binding to Tcf/Lef-family transcription factors and the general coactivator p300 using independent structural modules. *Mol. Cell* **10**, 573–584 https://doi.org/10.1016/S1097-2765(02)00631-7
98 Wu, G., Xu, G., Schulman, B.A., Jeffrey, P.D., Harper, J.W. and Pavletich, N.P. (2003) Structure of a beta-TrCP1-Skp1-beta-catenin complex: destruction motif binding and lysine specificity of the SCF(beta-TrCP1) ubiquitin ligase. *Mol. Cell* **11**, 1445–1456 https://doi.org/10.1016/S1097-2765(03)00234-X
99 Simonetta, K.R., Taygerly, J., Boyle, K., Basham, S.E., Padovani, C., Lou, Y. et al. (2019) Prospective discovery of small molecule enhancers of an E3 ligase-substrate interaction. *Nat. Commun.* **10**, 1402 https://doi.org/10.1038/s41467-019-09358-9
100 Kaieda, S., Matsui, C., Mimori-Kiyosue, Y. and Ikegami, T. (2010) Structural basis of the recognition of the SAMP motif of adenomatous polyposis coli by the Src-homology 3 domain. *Biochemistry* **49**, 5143–5153 https://doi.org/10.1021/bi100563z
101 Zhang, Z., Li, H., Chen, L., Lu, X., Zhang, J., Xu, P. et al. (2011) Molecular basis for the recognition of adenomatous polyposis coli by the discs large 1 protein. *PLoS ONE* **6**, e23507 https://doi.org/10.1371/journal.pone.0023507
102 Slep, K.C. (2012) Structure of the human discs large 1 PDZ2- adenomatous polyposis coli cytoskeletal polarity complex: insight into peptide engagement and PDZ clustering. *PLoS ONE* **7**, e50097 https://doi.org/10.1371/journal.pone.0050097
103 Day, C.L. and Alber, T. (2000) Crystal structure of the amino-terminal coiled-coil domain of the APC tumor suppressor. *J. Mol. Biol.* **301**, 147–156 https://doi.org/10.1006/jmbi.2000.3895
104 Tickenbrock, L., Cramer, J., Vetter, I.R. and Muller, O. (2002) The coiled coil region (amino acids 129–250) of the tumor suppressor protein adenomatous polyposis coli (APC). Its structure and its interaction with chromosome maintenance region 1 (Crm-1). *J. Biol. Chem.* **277**, 32332–8 https://doi.org/10.1074/jbc.M203990200
105 Zhang, Z., Akyildiz, S., Xiao, Y., Gai, Z., An, Y., Behrens, J. et al. (2015) Structures of the APC-ARM domain in complexes with discrete Amer1/WTX fragments reveal that it uses a consensus mode to recognize its binding partners. *Cell Discov.* **1**, 15016 https://doi.org/10.1038/celldisc.2015.16
106 Zhang, Z., Lin, K., Gao, L., Chen, L., Shi, X. and Wu, G. (2011) Crystal structure of the armadillo repeat domain of adenomatous polyposis coli which reveals its inherent flexibility. *Biochem. Biophys. Res. Commun.* **412**, 732–736 https://doi.org/10.1016/j.bbrc.2011.08.044
107 Morishita, E.C., Murayama, K., Kato-Murayama, M., Ishizuka-Katsura, Y., Tomabechi, Y., Hayashi, T. et al. (2011) Crystal structures of the armadillo repeat domain of adenomatous polyposis coli and its complex with the tyrosine-rich domain of Sam68. *Structure* **19**, 1496–1508 https://doi.org/10.1016/j.str.2011.07.013
108 Jiang, H., Deng, R., Yang, X., Shang, J., Lu, S., Zhao, Y. et al. (2017) Peptidomimetic inhibitors of APC-Asef interaction block colorectal cancer migration. *Nat. Chem. Biol.* **13**, 994–1001 https://doi.org/10.1038/nchembio.2442
109 Zhang, Z., Chen, L., Gao, L., Lin, K., Zhu, L., Lu, Y. et al. (2012) Structural basis for the recognition of Asef by adenomatous polyposis coli. *Cell Res.* **22**, 372–386 https://doi.org/10.1038/cr.2011.119
110 Dajani, R., Fraser, E., Roe, S.M., Young, N., Good, V., Dale, T.C. et al. (2001) Crystal structure of glycogen synthase kinase 3 beta: structural basis for phosphate-primed substrate specificity and autoinhibition. *Cell* **105**, 721–732 https://doi.org/10.1016/S0092-8674(01)00374-9
111 Sampietro, J., Dahlberg, C.L., Cho, U.S., Hinds, T.R., Kimelman, D. and Xu, W. (2006) Crystal structure of a beta-catenin/BCL9/Tcf4 complex. *Mol. Cell* **24**, 293–300 https://doi.org/10.1016/j.molcel.2006.09.001
112 Graham, T.A., Ferkey, D.M., Mao, F., Kimelman, D. and Xu, W. (2001) Tcf4 can specifically recognize beta-catenin using alternative conformations. *Nat. Struct. Biol.* **8**, 1048–1052 https://doi.org/10.1038/nsb718
113 Poy, F., Lepourcelet, M., Shivdasani, R.A. and Eck, M.J. (2001) Structure of a human Tcf4-beta-catenin complex. *Nat. Struct. Biol.* **8**, 1053–1057 https://doi.org/10.1038/nsb720
114 Graham, T.A., Weaver, C., Mao, F., Kimelman, D. and Xu, W. (2000) Crystal structure of a beta-catenin/Tcf complex. *Cell* **103**, 885–896 https://doi.org/10.1016/S0092-8674(00)00192-6
115 Sun, J. and Weis, W.I. (2011) Biochemical and structural characterization of beta-catenin interactions with nonphosphorylated and CK2-phosphorylated Lef-1. *J. Mol. Biol.* **405**, 519–530 https://doi.org/10.1016/j.jmb.2010.11.010
116 Graham, T.A., Clements, W.K., Kimelman, D. and Xu, W. (2002) The crystal structure of the beta-catenin/ICAT complex reveals the inhibitory mechanism of ICAT. *Mol. Cell* **10**, 563–571 https://doi.org/10.1016/S1097-2765(02)00637-8
117 Love, J.J., Li, X., Case, D.A., Giese, K., Grosschedl, R. and Wright, P.E. (1995) Structural basis for DNA bending by the architectural transcription factor LEF-1. *Nature* **376**, 791–795 https://doi.org/10.1038/376791a0
118 de la Roche, M., Rutherford, T.J., Gupta, D., Veprintsev, D.B., Saxty, B., Freund, S.M. et al. (2012) An intrinsically labile alpha-helix abutting the BCL9-binding site of beta-catenin is required for its inhibition by carnosic acid. *Nat. Commun.* **3**, 680 https://doi.org/10.1038/ncomms1680
119 Miller, T.C., Mieszczanek, J., Sanchez-Barrena, M.J., Rutherford, T.J., Fiedler, M. and Bienz, M. (2013) Evolutionary adaptation of the fly Pygo PHD finger toward recognizing histone H3 tail methylated at arginine 2. *Structure* **21**, 2208–2220 https://doi.org/10.1016/j.str.2013.09.013
120 Fiedler, M., Sanchez-Barrena, M.J., Nekrasov, M., Mieszczanek, J., Rybin, V., Muller, J. et al. (2008) Decoding of methylated histone H3 tail by the Pygo-BCL9 Wnt signaling complex. *Mol. Cell* **30**, 507–518 https://doi.org/10.1016/j.molcel.2008.03.011
121 Miller, T.C., Rutherford, T.J., Johnson, C.M., Fiedler, M. and Bienz, M. (2010) Allosteric remodelling of the histone H3 binding pocket in the Pygo2 PHD finger triggered by its binding to the B9L/BCL9 co-factor. *J. Mol. Biol.* **401**, 969–984 https://doi.org/10.1016/j.jmb.2010.07.007
122 Miller, T.C., Rutherford, T.J., Birchall, K., Chugh, J., Fiedler, M. and Bienz, M. (2014) Competitive binding of a benzimidazole to the histone-binding pocket of the Pygo PHD finger. *ACS Chem. Biol.* **9**, 2864–2874 https://doi.org/10.1021/cb500585s
123 Pickles, L.M., Roe, S.M., Hemingway, E.J., Stifani, S. and Pearl, L.H. (2002) Crystal structure of the C-terminal WD40 repeat domain of the human Groucho/TLE1 transcriptional corepressor. *Structure* **10**, 751–761 https://doi.org/10.1016/S0969-2126(02)00768-2
124 Jennings, B.H., Pickles, L.M., Wainwright, S.M., Roe, S.M., Pearl, L.H. and Ish-Horowicz, D. (2006) Molecular recognition of transcriptional repressor motifs by the WD domain of the Groucho/TLE corepressor. *Mol. Cell* **22**, 645–655 https://doi.org/10.1016/j.molcel.2006.04.024
125 Chodaparambil, J.V., Pate, K.T., Hepler, M.R., Tsai, B.P., Muthurajan, U.M., Luger, K. et al. (2014) Molecular functions of the TLE tetramerization domain in Wnt target gene repression. *EMBO J.* **33**, 719–731 https://doi.org/10.1002/embj.201387188

Biochemical Society Transactions (2020) **48** 1765–1780
https://doi.org/10.1042/BST20200243

126 Wang, H., Wang, Z., Tang, Q., Yan, X.X. and Xu, W. (2019) Crystal structure of the LUFS domain of human single-stranded DNA binding protein 2 (SSBP2). *Protein Sci.* **28**, 788–793 https://doi.org/10.1002/pro.3581
127 Wang, H., Kim, J., Wang, Z., Yan, X.X., Dean, A. and Xu, W. (2020) Crystal structure of human LDB1 in complex with SSBP2. *Proc. Natl Acad. Sci. U. S.A.* **117**, 1042–1048 https://doi.org/10.1073/pnas.1914181117
128 Yan, L., Xie, S., Du, Y. and Qian, C. (2017) Structural insights into BAF47 and BAF155 complex formation. *J. Mol. Biol.* **429**, 1650–1660 https://doi.org/10.1016/j.jmb.2017.04.008
129 Allen, M.D., Bycroft, M. and Zinzalla, G. (2020) Structure of the BRK domain of the SWI/SNF chromatin remodeling complex subunit BRG1 reveals a potential role in protein-protein interactions. *Protein Sci.* **29**, 1047–1053 https://doi.org/10.1002/pro.3820
130 Valencia, A.M., Collings, C.K., Dao, H.T., St Pierre, R., Cheng, Y.C., Huang, J. et al. (2019) Recurrent SMARCB1 mutations reveal a nucleosome acidic patch interaction site that potentiates mSWI/SNF complex chromatin remodeling. *Cell* **179**, 1342–56.e23 https://doi.org/10.1016/j.cell.2019.10.044
131 Farnaby, W., Koegl, M., Roy, M.J., Whitworth, C., Diers, E., Trainor, N. et al. (2019) BAF complex vulnerabilities in cancer demonstrated via structure-based PROTAC design. *Nat. Chem. Biol.* **15**, 672–680 https://doi.org/10.1038/s41589-019-0294-6
132 Papillon, J.P.N., Nakajima, K., Adair, C.D., Hempel, J., Jouk, A.O., Karki, R.G. et al. (2018) Discovery of orally active inhibitors of brahma homolog (BRM)/SMARCA2 ATPase activity for the treatment of brahma related gene 1 (BRG1)/SMARCA4-mutant cancers. *J. Med. Chem.* **61**, 10155–10172 https://doi.org/10.1021/acs.jmedchem.8b01318
133 Lolli, G. and Caflisch, A. (2016) High-Throughput fragment docking into the BAZ2B bromodomain: efficient in silico screening for X-ray crystallography. *ACS Chem. Biol.* **11**, 800–807 https://doi.org/10.1021/acschembio.5b00914
134 He, S., Wu, Z., Tian, Y., Yu, Z., Yu, J., Wang, X. et al. (2020) Structure of nucleosome-bound human BAF complex. *Science* **367**, 875–881 https://doi.org/10.1126/science.aaz9761